The Power of Field Measurements – Part I

Conveyor Dynamics, Inc., personnel, USA

Summary

This article describes current test methodologies and equipment used for field measurements of long overland belt conveyor systems. A comparison is made between the theoretical calculations and field measurement results. It is shown how field measurements can be used to determine deviations from the actual system performance as compared to the expected design performance. Accurate theoretical performance prediction of the belt's power, strength and life expectancy are becoming important design tools as the belt conveyor's share of the project capital and operating expenses become significant. Accurate measurement is the only true method of validating the theory and therefore assumes special significance in certifying the accuracy of theoretical models. Inaccurate predictions lead to either a serious risk of failure or wasteful and excessive expenditure of the client's capital and operating cost.

1 Introduction

Many articles have been published in this magazine on both analytical and numerical methods to design long overland belt conveyor systems. Only a few papers discuss the actual performance of the system once it has been erected and commissioned. This article will describe the test methodology, equipment and some measurements acquired by Conveyor Dynamics, Inc. (CDI) during commissioning of long overland belt conveyor systems. It will demonstrate the power of acquiring field measurements to determine deviations from the actual system performance as compared to the expected performance described in the design report. Changes from the design settings of system components (brakes or drive controllers for example) can result in serious operational problems. To fully understand the cause of these problems, and provide an appropriate solution, it is important to understand the theoretical background of the dynamics of a belt conveyor system. A comparison is then made between the theoretical calculations and certain field measurements. Only a part of the available field measurements will be described in Part I of this article. Part II will include a description of belt side travel, conveyor component noise, belt flap, and acceleration measurements.

2 The conveyor system

CDI was commissioned by Barclay Mowlem to deliver the mechanical design of the Muja power station designated belt conveyor P2 for the Western Power Corporation (WPC), see Figure 1. Muja power station is located in Western Australia near the town of Collie. Conveyor P2 is the longest of a series of conveyors that transport coal from the coal fields to Muja power station. The conveyor is approximately 6.1 km long and has an overall elevation increase of approximately 15 m from the tail to the head pulley, see Figure 2. The conveyor has 29 vertical curves, 14 concave and 15 convex curves. The minimum radius of the concave curves is 1500 m and 800m for the convex curves. The conveyor also has one large horizontal curve with a radius of 4500 m.

The design report was finished in January 1997 and the field measurements were performed during the commissioning in January 1998.

Figure 1: *Beginning of the horizontal curve for Muja power station conveyor P2*

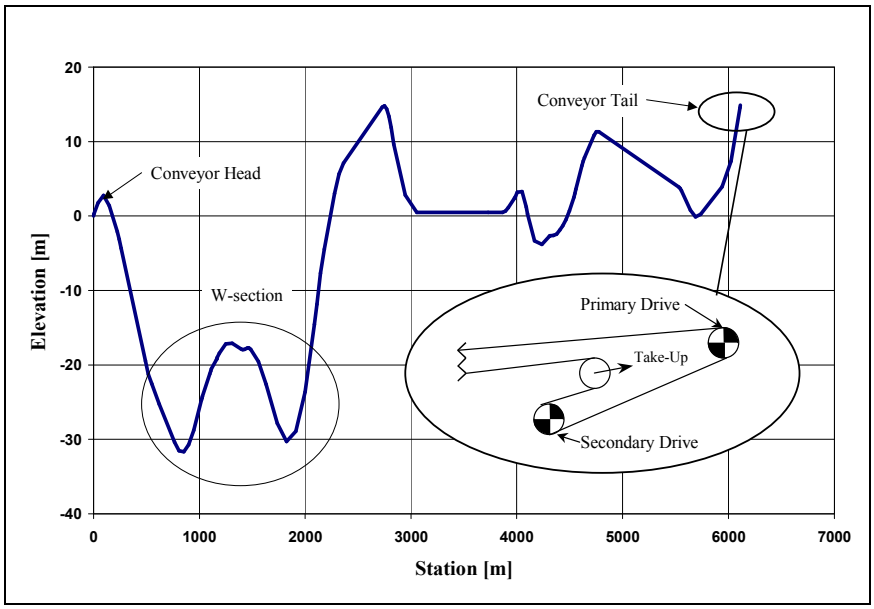

Figure 2: *Profile for P2 conveyor*

The major design specifications of conveyor P2 are:

Material ..... Coal
Capacity ..... 770 T/H, density 850 kg/m^3, surcharge angle 20 °
Belt ..... ST 800 N/mm, 800 mm wide
Motors ..... 2 x 315 kW dual drive arrangement at head

3 Computational design tools

Steady state and dynamic analysis methods were used to determine belt power, tension levels, and starting and stopping control methodologies. For steady state analysis the belt is assumed to act as a rigid (inelastic) body. The dynamic analysis uses a two dimensional wave theory to determine the time dependent propagation of tension waves through the belt. For dynamic analysis, the belt is divided into a series of elements containing elastic springs, dashpots, and discrete masses, see Figure 3. For the symbols used in that figure it is referred to [3]. Rheological laws determine the interactions between these elements. Large amplitude tension waves, sometimes referred to as "shock waves", and large local belt displacements can only be resolved using dynamic analysis

Steady state analysis produces the running belt tensions and power consumption for all material loading conditions and temperature variations. A computer program, tradenamed BELTSTAT, is used to analyze the steady-state design. Dynamic analysis produces the belt tension and the power consumption during non-stationary operation of the belt conveyor, like starting and stopping. Dynamic analysis is performed with a computer program tradenamed BELTFLEX.

Dynamic analysis is used to:

a. Simulate all motor and brake (if any) starting and stopping control functions and integrate their independent control methods with the belt's elastic response.
b. Develop control strategies and dynamic tuning methods (if required) to limit variations in belt tension and displacement within acceptable levels.
c. Analyze and control the cause and effect resulting from "what if" operation scenarios such as drive and brake malfunctions.

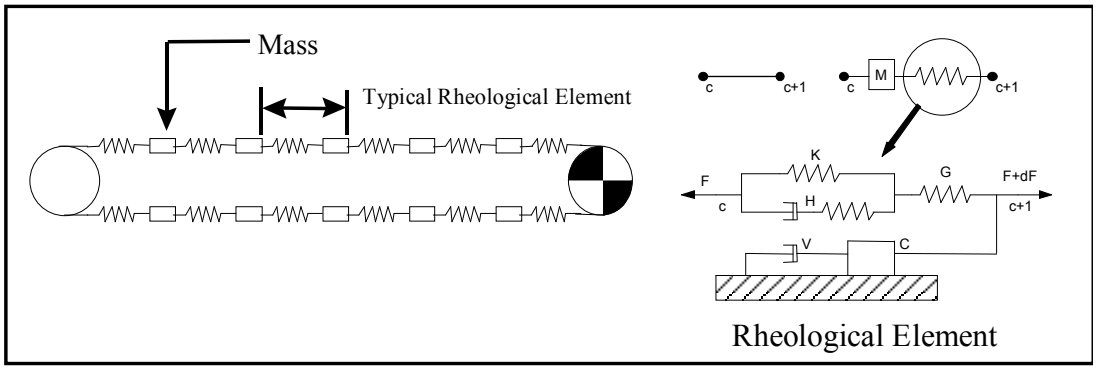

Figure 3: *Example of a finite element representation of the belt conveyor and the belt*

4 Design specifications

The company that designs a long belt conveyor system may not manufacture it. If designer and manufacturer are the same, the client often contracts a consultant to audit their work. Either the designer or the consultant may request field measurements. The main reasons for field measurements are to confirm that a system has been built in accordance with the design specifications and performs as predicted by the designers.

The design report is used as the basis for comparison of the field measurements to the design specifications. Typical specifications made in a design report include:

1. Material: tonnage, density and surcharge angle
2. Belt: width, strength, cover thickness, mass, Young's modulus, speed, trough configuration
3. Drive assembly: power rating, RPM's, inertia's, number of drives, locations, efficiencies, gear box ratios
4. Holdbacks: size, number and locations
5. Flywheels: size, number and locations
6. Take-up system: location, required belt line tension at take-up pulley, total required take-up displacement
7. Idlers: idler spacing, roll sizes, applied loads, quantities
8. Pulleys: arrangement, sizes and belt line tension at pulley locations
9. Curves: sizes, belt stresses in curves, lift-off analysis
10. Belt flap analysis
11. Starting control
12. Stopping control, including sequential regulation between connecting conveyors

Today, clients may request the supplier of a long belt conveyor system to guarantee that the system can be built at minimum capital and operational cost. They may also request a specification of the efficiency to transport the material at the design tonnage over the projected route and the maximum replacement rate of system components, such as idlers and belting. It should therefore be realized that the values of the system parameters, as given in a design report, are design values. These values may differ from the expected values as follow from the design calculations. The margin between the design and the expected values depends on the accuracy of the computational design tools, their input parameters, and the experience of the supplier. A typical expected percentage between the design and the expected values of system parameters is 10%. This level of accuracy is rarely achieved in overland conveyor design due to inaccuracy of the computational design tools, which are referenced to common standards.

5 Test Procedures & Equipment

Most major conveyor components such as drives, brakes, and take-up systems are located at the head and tail of the system. Because of this, most of the measurements are conducted at these locations. Unfortunately, these are areas of severe voltage and current fluctuations, as well as heavy EMF influences. For these reasons, all of the data acquisition equipment used in the field must be extremely robust. It has to be capable of not only withstanding large voltage fluctuations and transients, but it must be reliable, portable, and extremely noise immune.

The following is a brief introduction to some of the equipment and methods used by CDI to acquire data for large overland conveyor systems. When relevant, attention has been given to the accuracy of the measurement and/or equipment.

5.1 Data Acquisition Recorder

The basis of all of the field equipment is the data acquisition recorder. This device digitizes the various transducer signals, which can then be recorded on a notebook computer. A single data acquisition recorder may be used simultaneously to record more than 50 signals.

Sample rates depend on the rate at which the signal changes in time and the desired accuracy of the result. Typically, sample rates vary between 0.1Hz to 10kHz. High sampling rates are for example required to adequately capture motor and brake torque transients, velocity changes caused by transient stress waves, take-up motion, motor contactor response, brake valve and caliper timing, etc. Low sampling rates are used for recording weight scale and temperature measurements.

To ensure proper timing for each field test, all data recording units must be "triggered" or started simultaneously. Since overland conveyors often transverse vast terrain, this is difficult at best. If PLC signals are available at both ends of the conveyor, a push button trigger signal can be hardwired into the PLC. This signal can then be relayed to the other end of the conveyor and all data recorders started simultaneously. This typically results in less than a 50ms delay. Other methods include a verbal countdown (if communications are available), or both users triggering at predefined intervals.

Two types of testing methods can be preformed. The first is a "static" method. For this method all data recorders are triggered simultaneously. Data is recorded at a fixed sampling rate for a preset set time interval. For example, a 60-second test with a sampling rate of 10 Hz may be used to capture a startup or shutdown of the conveyor system. Unfortunately this method requires prior knowledge that the conveyor is indeed starting or stopping and the data recorder must be triggered before the event occurs. Although high sampling rates may be required during starting and stopping of the conveyor, these rates are not desirable for long term testing. The drawback of this method is the enormous amount of data that may be recorded due to high sample rates and long time intervals. The second method, which solves this problem, is a "dynamic" testing method which allows high sampling rates during transition periods and low sampling rates during steady state and shutdown periods. For this method, the data recorders are set to sample at the highest sampling rate desired. They are then all triggered simultaneously. After a specified time interval, say 500 seconds, the recorded data is analyzed. If the velocity of the conveyor has changed significantly, (the conveyor is started or stopped) then the data in this interval is saved to a time stamped file. If the velocity has not changed (the conveyor is either not moving or at steady state) then the power, temperature, and/or other steady state quantities can be time averaged and saved to a separate data file. This method is far more complicated than the static test method, but it allows long term testing to be preformed without any user intervention. It also gives the engineer the ability to capture unexpected conveyor shutdowns.

5.2 Conveyor belt velocity

One of the most fundamental of all field measurements is that of belt velocity. Not only is this measurement necessary to confirm that the conveyor is indeed operating at its design speed, but more importantly to verify the starting and stopping dynamics of the overall conveyor system. Currently, the two most popular methods for determining conveyor velocity are by using either a magnetic pickup sensor or an optical encoder.

Magnetic pickups require a rotating metal plate or gear tooth from which they received a pick signal or "pulse". These devices may have as few as 1-32 pulses per revolution. Although the errors produced from these devices may be acceptable at steady state velocity, their accuracy is severely diminished at low speeds. Since velocity is often used as a feed back signal to the PLC when starting and stopping the conveyor these errors may be significant. For example, a magnetic pickup device with only 16 pulses per revolution, mounted on an 1800mm diameter pulley rotating at 5.6 rad/s (belt speed is 1 m/s), will only produce 1 pulse every 350ms. Optical encoders on the other hand use an etched glass disk, which is rotated through a photoelectric diode. These devices can easily contain over 2,000 pulses per revolution. For the example above, an optical encoder and corresponding tachometer mounted on the same system would produce 1 pulse every 3ms. Furthermore, unlike magnetic pickups, optical encoders can output a dual quadrature signal, resulting in doubling the signal count per revolution. This provides higher noise rejection, the ability to infer the rotational direction, and a more accurate signal.

A typical optical encoder assembly is shown in Figure 4. An optical encoder and wheel assembly is mounted on a movable aluminum arm and fixed to the structure.

Figure 4: *Velocity Encoder and wheel*

Velocity encoders can be used in conjunction with one another as shown if Figure 5. Here two velocity encoder units are used to measure possible belt slippage. One unit is mounted on the belt, and measures the actual (angular) belt speed. The other unit is mounted on the pulley lagging to measure the (angular) pulley speed. Any velocity difference between these two, taking into account the difference in radii, is an indication of belt slip (also see Section 6.3).

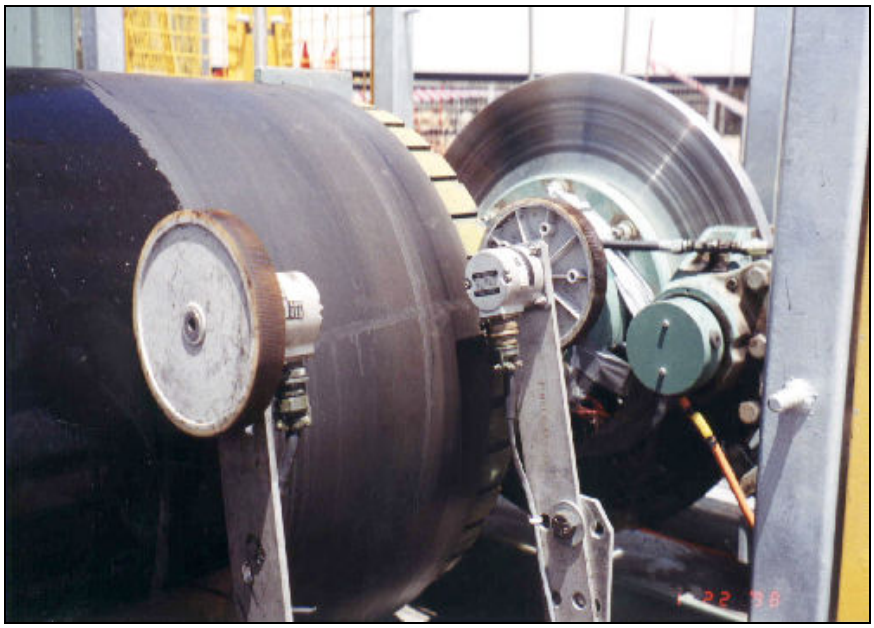

Figure 5: *Two encoders mounted on a brake pulley to observe potential belt slip*

5.3 Conveyor Power & Motor Torque

Accurate power measurements must be taken to verify the outcome of the steady state calculations, confirm that a sufficient amount of power has been installed, and identify the accuracy of the design. There are three common methods for measuring conveyor power at the drive pulley low speed shaft. The first method is to use a power transducer (watt meter). A power transducer measures the current and voltage going into a drive system. This is then be converted to a motor power. Unfortunately, the power measured in this manner includes electrical and mechanical losses in the motor, gearbox, fluid coupling, and/or other losses. An engineering guess must therefore be made as to the exact losses of each of these components to determine the actual power consumed by the conveyor belt itself. The second method is to measure the motor RPM, and use this in conjunction with a motor slip power curve. This method however, is only applicable for specific drives types. Furthermore, since this method includes the losses from the gearbox, fluid couplings, and other intermediate equipment, the conveyor power at the drive pulley low speed shaft cannot be directly determined.

The third method for measuring conveyor power is by directly measuring the strain in the drive pulley shaft caused by the applied torque. This deformation can then be directly converted to drive torque. The torque is then multiplied by the conveyor's velocity and divided by the pulley's radius to obtain the conveyor's power. Figure 6 shows the equipment necessary for acquiring accurate torque measurements. Strain gauges are mounted on the gearbox and/or pulley shaft. Due to the shaft's rotation, wires cannot be directly connected from the data acquisition equipment to these gauges. Instead, either slip rings or wireless methods must be used. Slip rings are typically unacceptable for these types of applications because they produce excessive noise and the physical

geometry of the system often does not allow their installation. Wireless methods have proven to be acceptable and very reliable. A small battery powered transmitter and transmitting antenna is mounted on the rotating shaft. The transmitter functions as both the power supply and amplifier for the strain gauge bridge mounted on the shaft. It then converts the strain gauge output into a 5kHz pulse modulated FM signal. This signal is transmitted to a stationary-receiving antenna fixed around the outside of the shaft. The receiving antenna is then connected to a receiver unit, which converts the FM signal back into a DC voltage. The data acquisition recorder then acquires this voltage.

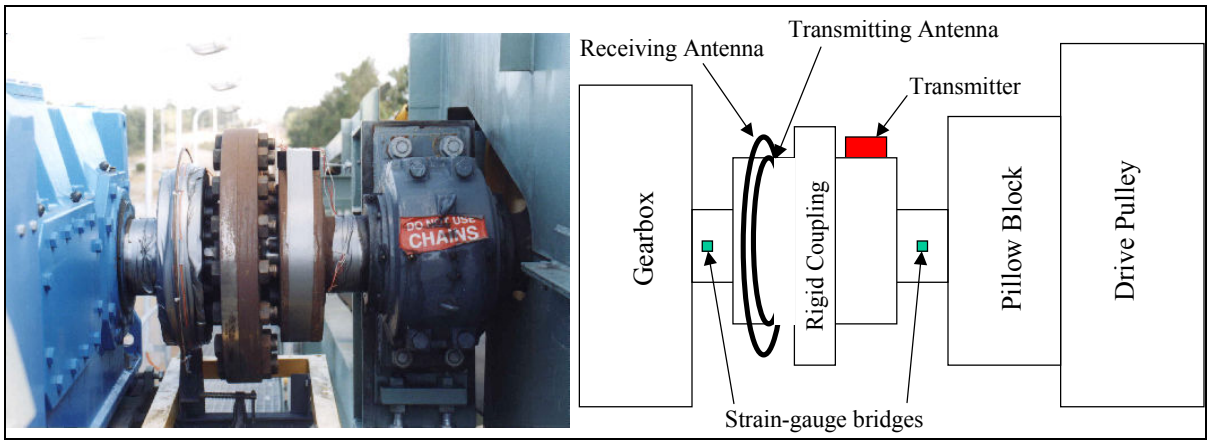

Figure 6: *Strain gauge assembly used to measure shaft torque & conveyor power*

Figure 7 shows a typical result of torque measurements from a wound rotor motor startup. The holdback and steady state torques are shown. Furthermore, each of the 25 resistor steps and their corresponding firing sequence can be identified.

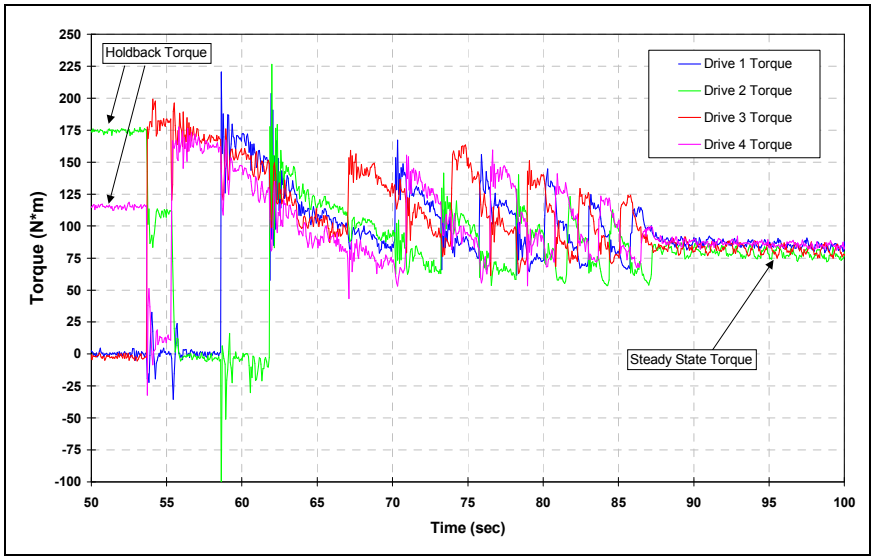

Figure 7: *Torque measurement for a wound rotor motor startup*

An interesting side result can be obtained by performing a Fast Fourier Transformation (FFT) of the steady state torque signals. From the raw torque signal a vast amount of information about the system can be determined.

Figure 8 shows the system configuration and results from an FFT performed on a steady state torque signal. This system consisted of a squirrel cage motor, fluid couplings, gearbox, and drive pulley. A strain-gauge bridge was mounted on the shaft between the gearbox and drive pulley. The x-axis of Figure 8 has been converted from a frequency spectrum to an equivalent shaft RPM speed. Due to a small misalignment in the drive system, the high frequency torque components of the fluid coupling were transmitted, through the gearbox to the pulley shaft. These components are shown in Figure 8. These frequency components allowed the slip across the fluid couplings to be calculated. Furthermore, by knowing the motor RPM, the torque could be back calculated from a motor slip curve. This torque agreed within 3% of the actual measured torque. Additionally, the pulley shaft RPM was clearly present, and the conveyor velocity could be calculated. This agreed within 5% of the measured velocity. The remaining frequency spikes correlate to the gearbox reduction steps and their higher harmonics.

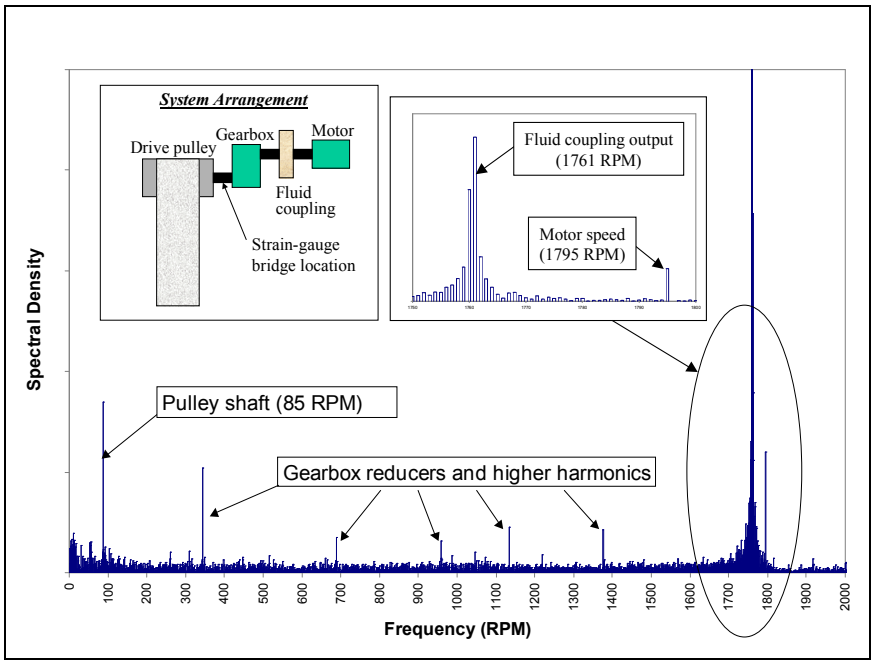

Figure 8: *Fast Fourier Transform of a raw torque signal*

5.4 Take-up tension

From the results of torque measurements, the tension differential over the drive pulley is known. To obtain the actual tension values one of the two tensions has to be known as a reference. The most convenient tension to measure is the take-up tension. This tension is later used as a *reference* tension.

The take-up tension is usually measured using a load cell installed in the cable arrangement of the take-up system. If possible a pre-made and calibrated load cell is used. In that case the error made in the tension measurement is less than 1%. Otherwise, the take-up structure itself may be strain-gauged and used as a load cell. Figure 9 shows a load cell installed at the terminating end of the gravity take-up cables of the Muja P2 Conveyor.

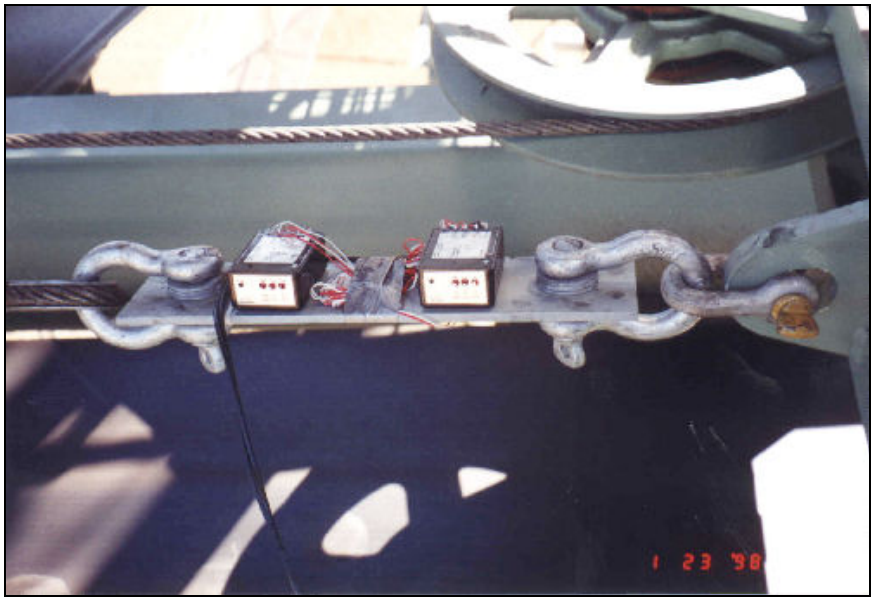

Figure 9: *Load cell installed on gravity take-up system*

5.5 Take-up displacement

Take-up displacement is measured to verify its theoretical prediction and confirm the take-up displacement requirements.

Take-up displacement is measured with the same equipment used for measuring conveyor velocity. In this case however, the dual quadrature pulse is counted in time to provide an equivalent displacement instead of velocity. A typical displacement apparatus mounted on a take-up sheave is shown in Figure 10. The accuracy of the assembly is approximately ±5mm over a 1,000mm displacement range. This is less than 0.5% and well within the desired precision.

Figure 10: *Take-up Displacement Measurement*

5.6 Temperature

Ambient temperature variations can significantly alter the visco-elastic properties of the conveyor belt's cover rubber compound. These variations are usually given a design parameter and accounted for in the steady state analyses. Temperature variations affect the rubber deformation as it travels over the idlers, which in-turn changes the power consumption of the conveyor. Low temperatures can also increase the idler bearing drag. When elevation changes of a conveyor are significant, temperature measurements are acquired at both the head and tail of the conveyor system. Temperature measurements are continuously acquired using a thermocouple and recorded by the data acquisition recorder during each test. In some cases both summer and winter testing must be conducted to confirm the power fluctuations with temperature of the conveyor system.

5.7 Brake Torque

Brake torque measurements are required to verify that the brake system is performing in accordance to the manufacturer and design specifications.

Brake torque is measured using the same techniques as motor torque. A typical arrangement for measuring brake torque on a decline conveyor system is shown in Figure 11. For this system the brake is located between the output shaft of the gearbox and the conveyor's tail pulley. Although only one side of the disk brake is shown, both sides have been instrumented with strain-gauge bridges.

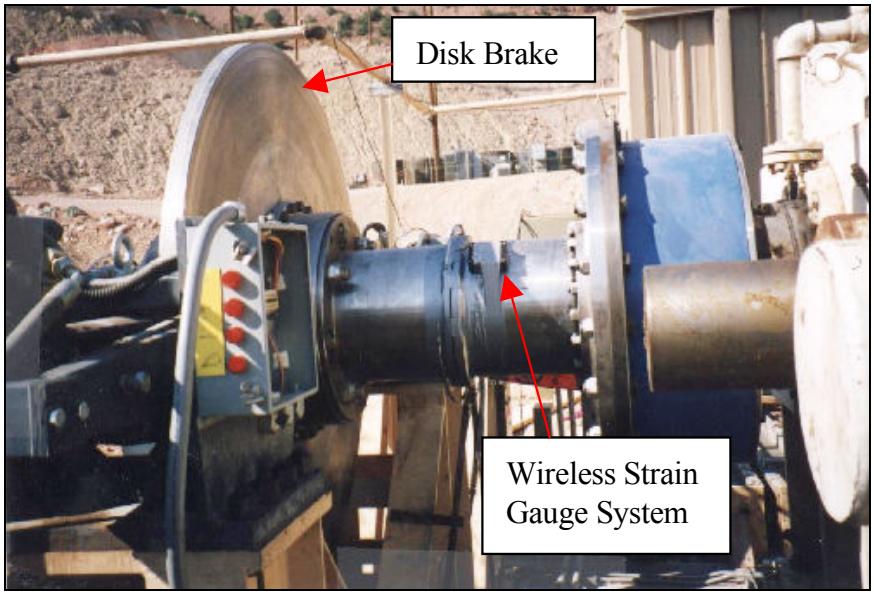

Figure 11: *Disk Brake Torque Measurements*

Figure 12 shows the brake torque results from an operation stop of the system shown in Figure 11. The stop is initiated 6 seconds into the test. Prior to that time, the conveyor is running at steady state conditions where the regenerative power of the conveyor can be calculated. Note that the two torque signals (which are on two different shafts with different shaft diameters and wall thickness) are within 2% variation of each other. After 6 seconds, the brake is applied. Part of the brake torque is utilized to stop the conveyor while the rest is used to stop the motor and flywheel. Strain-

gauge bridges on both sides of the brake disk allow each torque component to be determined separately. These components can then be added together to obtain the total brake torque.
The overall error in of the torque measurement is determined by the errors made of the speed measurements (<1%), the torque measurement (<2%) and the parameters of the shaft material (<2%). This results in an overall error of less than 5%.

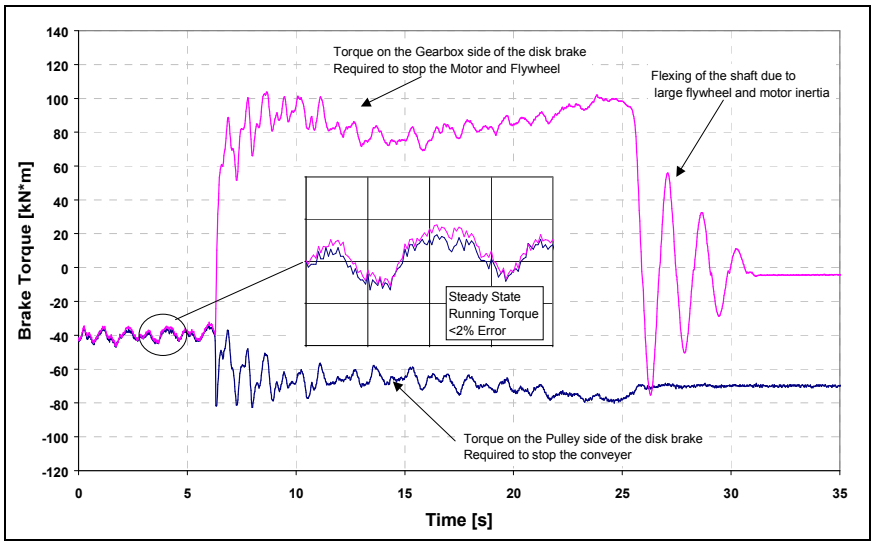

Figure 12: *Brake disk torque results and measurement error*

5.8 Weight Scale

It is important that the exact belt load ins known to enable an accurate comparison between the results of the steady state and dynamic analyses to the results of the measurements. Precise weight scale readings must therefore be recorded. Fortunately, most long overland conveyors already have calibrated weight scales installed during commissioning. In this case the signal and appropriate scaling factors can be taken directly from the PLC. It is important to realize that when acquiring measurements, the bulk material load on the belt is not the same as the current weight scale readings. In order to determine the correct loading profile on the belt, both weight scale and velocity must have been recorded for a certain period prior to the test. The length of this period must be at least the conveyor length divided by the steady state velocity. The loading values can then be integrated over the entire length of the conveyor to determine the actual belt load.

6 Muja: Theory & Practice

In this section a comparison will be made between the theoretical prediction and the results of the field measurements as acquired for Muja conveyor P2.

6.1 Power consumption

As already mentioned in the Section 3, clients may request a specification of the minimum efficiency, for example quantified in terms of maximum kW-hr/ton/km, to transport the bulk solid material at the design specifications over the projected route. For long overland conveyor systems, the transport efficiency is mainly determined by the indentation rolling resistance [1]. It is therefore very important that design tools are available to accurately calculate the belt's indentation rolling resistance. Some of the design tools used by CDI have previously been described before in [2] and [3], and the applicable theory in [4].

Figure 13 shows a comparison between the measured and the predicted power consumption of the Premier Muja belt conveyor P2. It also shows the expected power consumption as determined by the conventional CEMA method [5]. Commissioning was performed during the summer and the figure is therefore only valid for these conditions (27° centigrade).

The dash-dotted line in Figure 13 shows the design values of the power consumption, as given in the design report issued in 1997. These numbers are conservative as explained in Section 4. CDI's criteria is to provide a 10% reserve over the expected power draw for the long term changes to belt, structural alignment, and load sharing drift (pulley wear etc.). The solid line reflects the expected values of the power consumption as yielded from the design calculations. The maximum difference in power between the design power and the expected power is about 25 kW (less than 10%). The average deviation between the expected and the actual measured values of the power is 4.3%. This falls within the accuracy of the measurements. The average deviation between the design values and the measured values is less than 15%.

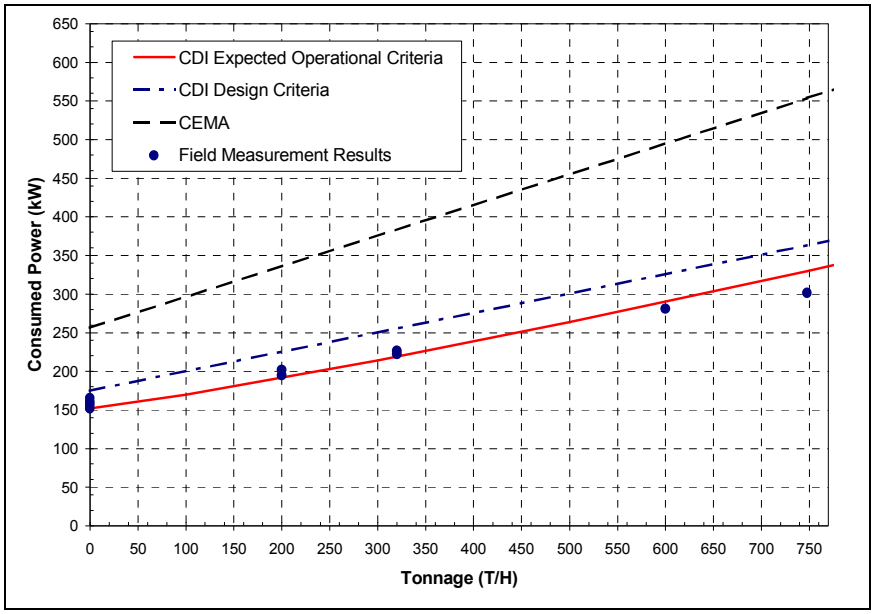

Figure 13: *Comparison between measured and predicted power consumption of conveyor P2*

The required drive power of a conveyor is determined by the sum of the total frictional resistances and the total material lift. The frictional resistances include hysteresis losses, which can be considered as a viscous (velocity dependent) friction component. It does not suffice to look just at the maximum required drive power to evaluate whether or not the power consumption of a conveyor system is reasonable. The best method to compare the power consumption of different systems is to compare their transport efficiencies.

There are a number of methods to compare transport efficiencies. The first and most widely applied method is to compare equivalent friction factors such as the DIN f factor. For P2 that factor is 0.013 with the fully loaded belt (770 T/h). An advantage of using an equivalent friction factor is that it can also be determined for an empty belt. A drawback to using an equivalent friction factor is that it is not a "pure" efficiency number. It takes into account the mass of the belt, reduced mass of the rollers and the mass of the transported material. However, in a pure efficiency number, only the mass of the transported material is taken into account. The second method is to compare transportation cost, either in kW-hr/ton/km or in $/ton/km. For the Muja conveyor P2, the transportation cost for a fully loaded belt is 0.072 kW-hr/ton/km. The advantage of using the transportation cost is that this number is widely used for management purposes. The disadvantage of using the transportation cost is that it does not directly reflect the efficiency of a system. The third and most "pure" method is to compare transport efficiency numbers. The transport efficiency number is the ratio between the drive power required to overcome frictional losses (neglecting drive efficiency and power loss/gain required to raise/lower the material) and the transport work. The transport work is defined as the multiplication of the total transported quantity of bulk solid material and the average transport velocity. For the Muja P2 conveyor the transport efficiency number is 0.025. This number can for example be used to compare the transport efficiencies between a belt conveyor and a truck system. The disadvantage is that it depends on the transported quantity of material and thus cannot be determined for an empty conveyor.

6.2 Wave propagation speed

The belt's elastic properties and the mass of the belt, idlers and bulk material mainly determine the dynamic behavior of long belt conveyor systems. The speed at which stress-waves travel through the belt must be known to determine appropriate starting and stopping procedures. Two wave speeds can be distinguished: the longitudinal wave speed and the propagation speed of transverse waves [6]. The longitudinal wave speed is determined by the belt's Young's modulus, the cross sectional area of the belt, the mass of the belt and bulk material, and the reduced mass of rollers.

The expected longitudinal wave speed in a belt can be theoretically calculated if the belt parameters are known [6]. The actual wave speed can be determined from measuring the time it takes a tension wave to travel from the head to the tail of the conveyor. The most suitable measurement to determine the wave speed is to measure the belt speed at the head and at the tail of the conveyor during an emergency stop. During an emergency stop the drives are switched off, the belt tension at the head drops considerably and a sudden change in belt speed at the head occurs.

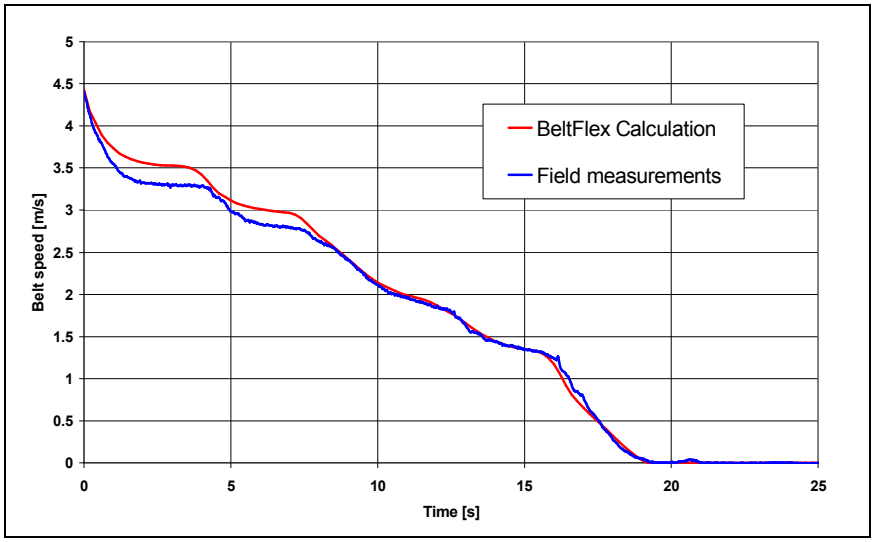

Figure 14: *Belt speed at the head of the conveyor. The belt is empty*

Figure 14 shows the velocity of the belt at the head of the conveyor as calculated by BELTFLEX, and as measured on site. At t=0 s the drives are switched off and the belt speed drops down from 4.4 m/s to 3.5 m/s. Figure 15 shows the belt speed at the tail of the conveyor. At t=0 the tail brake is applied which causes a small decrease in belt speed. At t=3.1 s the tension wave coming from the head arrives at the tail of the conveyor and the belt speed drops down to 2.8 m/s. This time lag is 3.1 seconds. Dividing the length of the 6.1 km conveyor by the time lag, yields the wave speed. In this case the wave speed is 1968 m/s which is a representative number for an empty steel cord belt. This wave speed is used as a *reference*.

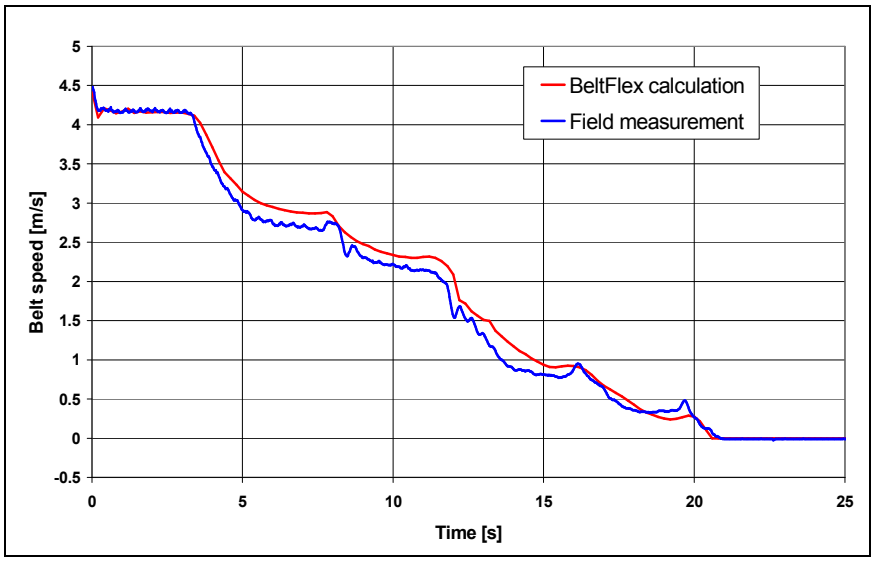

Figure 15: *Belt speed at the tail of the conveyor. The belt is empty and a tail brake is applied*

Using the (measured) belt's Young's modulus of 5154 N/mm^2, and the belt density of 1307 kg/m^3, a theoretical longitudinal wave speed of 1985 m/s can be calculated. This is within 1% of the measured wave speed. When calculating the wave speed for a loaded belt, a part of the reduced mass of the rollers and the belt load has to be taken into account. As the belt is loaded the wave speed will decrease. Figure 16 shows the decrease in wave speed as a ratio of the actual wave speed (as determined from the measurements) and the *reference* wave speed. The upper line shows

the theoretical wave speed decay only taking into account the mass of the material and belt. The lower line shows the wave speed decay taking also the reduced mass of the rollers into account. For both lines 100 % of the material mass is taken into account. The dots in Figure 16 show the wave speed ratios as determined from the actual field measurements at different tonnages. It can be observed that the contribution of the reduced mass of the rollers becomes more prevalent as the belt load increases. The slip between the belt and the idler rolls, which may occur during passage of a transient stress wave, decreases with increasing belt load.

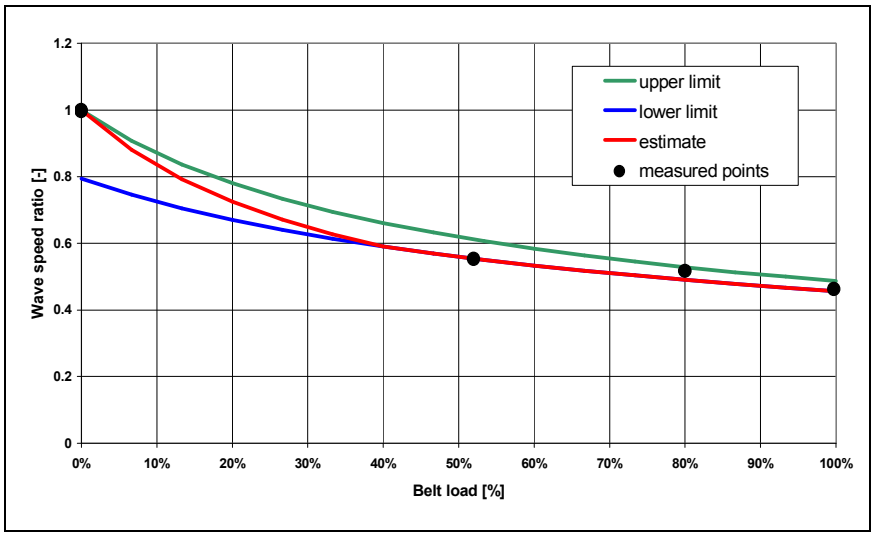

Figure 16: *Decrease in wave speed ratio with increasing belt load*
A belt load of 100 % is the belt loaded at the design tonnage

6.3 Dynamic tuning

The process of determining the settings of the drives, brakes and/or flywheels is called dynamic tuning of the system. A 10 kNm brake is applied during an emergency stop to both limit the stopping time and prevent excessive belt sag in the carry strand of the conveyor's W-section, also see Figure 2. The tension at the head of the conveyor quickly drops to the pre-tension when the drives are switched off. This tension drop generates a negative tension wave in the carry strand travelling from the head of the conveyor, to the tail of the conveyor, and to the drive/take-up station lowering the tension in the whole belt. If the brake is not applied, the conveyor will drift to a stop and the tensions in the W-section of the belt will fall below an acceptable level, yielding more than 5% of belt sag. A tail brake is required to increase the belt tension during an emergency shut down. The carry strand tension is increased as soon as the brake is applied generating a positive tension wave travelling from the brake pulley towards the head of the conveyor increasing the tension in the carry strand of the belt. If the brake is located at the tail, the positive tension wave arrives in time at the W-section to counteract the negative tension wave coming from the drive stations. If the brake is located at the head, it arrives too late regardless of brake size. The disadvantage of having the brake at the tail pulley is that the tension in the return strand of the belt can also be very low during an emergency stop. These low tensions may yield a very high tension-ratio over the brake pulley, which could result in belt slippage. In practice, the tension ratio is limited by the friction between the belt and the pulley, and the wrap angle. The belt will start to slip on the pulley as soon as the maximum tension ratio is reached. A capstan was installed at the take-up for this reason. The function of a capstan is to limit the take-up motion thereby not allowing the belt to relax. This results in a relatively high tension level in return strand of the belt.

The capstan is designed to increase the belt tension by 22.5 kN. The pre-tension of the belt is 30 kN.

During commissioning, it was observed that the belt slipped on the brake pulley during an emergency stop. The belt and brake pulley (Figure 17), the tail brake torque (Figure 18), and the take-up tension (Figure 19) were measured to determine the cause for the slippage. Figure 17 shows the belt speed at the head and the tail of the conveyor during an emergency stop. The green line shows the belt speed at the head, the blue line the belt speed at the tail and the red line shows the (angular) speed as measured on the brake pulley. The belt starts to slip on the brake pulley about 9 seconds after initiation of the emergency stop. Figure 18 shows the brake torque during the emergency stop. From this figure it can be seen that the torque applied by the brake was 6 to 8 kNm instead of the design value of 10 kNm. The brake therefore did not cause the slippage problem since the tension ratio decreases with decreasing brake torque. Figure 19 shows the variation in take-up force and take-up displacement during an emergency stop. This figure shows that the capstan increased the belt tension only by 4 to 5 kN instead of the design value of 22.5 kN. This implies that the tension before the brake pulley was much lower then intended, and therefore the tension ratio was much higher than expected. The malfunctioning of the capstan therefore was the reason of the slippage of the belt on the brake pulley.

Although the tension ratio cannot be measured directly, it can be resolved using BELTFLEX. Using the lower capstan force, BELTFLEX predicted the tension levels as shown in Figure 17. From that figure it can be observed that the belt starts to slip as soon as the tension ratio exceeds 5. With a wrap angle of 180° the maximum friction coefficient between the belt and the ceramic lagging can be calculated to be 0.5. This is much lower than the value of about 0.8 as specified by the lagging manufacturer. The field measurements have shown that the friction factors for ceramic lagging can only be safely used for high tension pulleys (drive pulleys). For low tension pulleys (tail/brake pulleys) the actual friction factor is much lower.

To complete the picture: Figure 20 shows the drive torque of the two drives. As can be seen the load sharing is about 1:1.16. The drive torque visible at the end of the stopping cycle is caused by application of the holdbacks.

This example shows that changes from the design settings of system components (brakes or drive controllers for example) can result in serious operational problems.

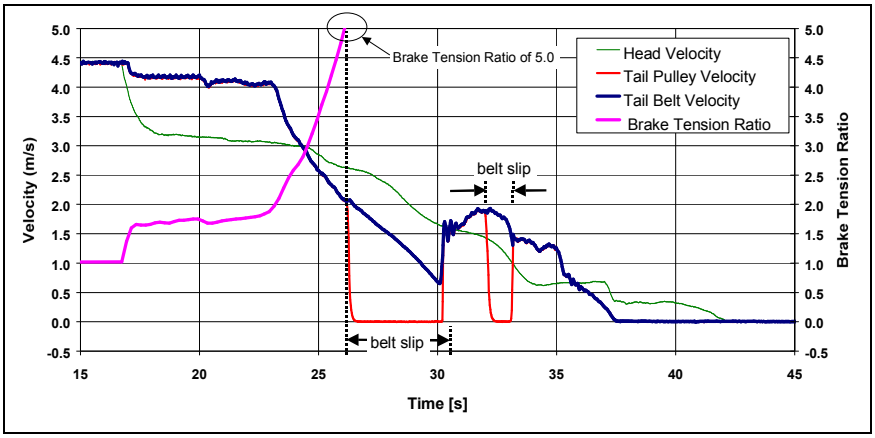

Figure 17: *Belt speed at the head and the tail of the conveyor and the tension ratio on the brake pulley during an emergency stop*

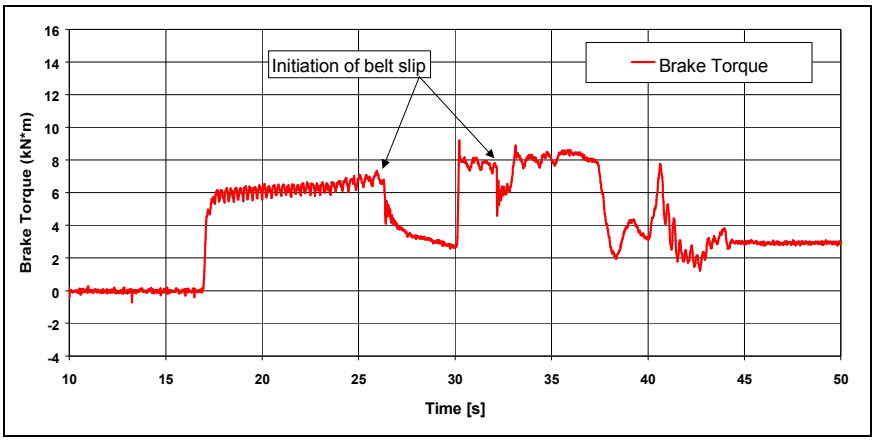

Figure 18: Brake torque during an emergency stop

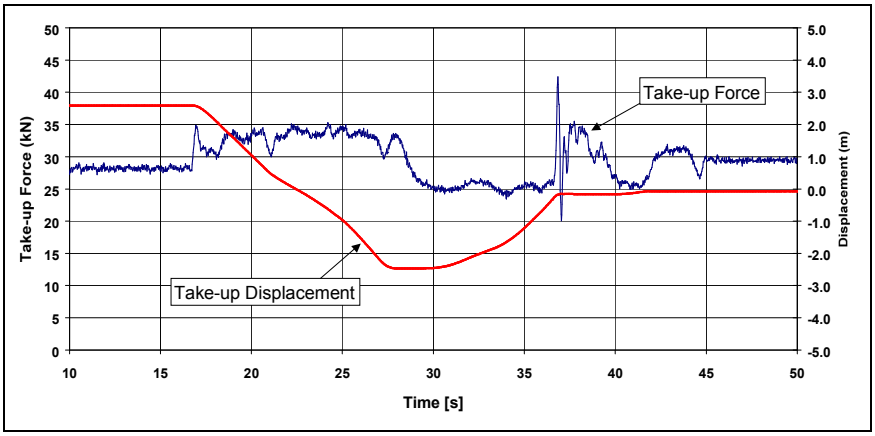

Figure 19: *Variation in take-up force and take-up displacement during an emergency stop*

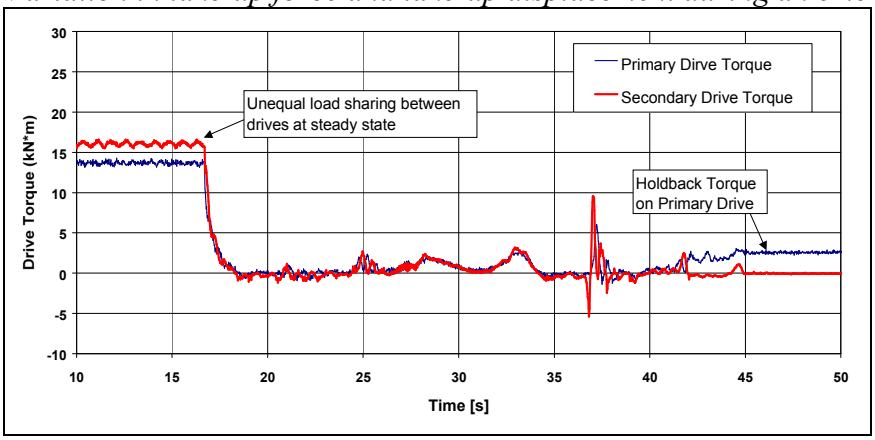

Figure 20: *Drive torque during an emergency stop*

7 Conclusions

1. A design report is used as the basis for comparison of field measurements to the design specifications. The specifications in that report should therefore be complete and clear.
2. Today, the test methodologies and the equipment is available to accurately acquire all field measurements required for the commissioning of long overland conveyor systems. Understanding the theoretical background of the dynamics of belt conveyors is required to analyze the results of field measurements.
3. Comparison of the results of field measurements to the results of steady state and dynamic analyses shows that the results of calculations performed with BELTSTAT and BELTFLEX are accurate. The deviation between the measured and the expected (calculated) values of system parameters is less then 5%. This falls within the accuracy of the field measurements.
4. Field measurements are required for forensic engineering. Even though steady state and dynamic analysis can be used to determine a possible cause for operational problems, field measurements are required to determine the actual settings of system parameters.

8 Acknowledgements

The authors like to extend their gratitude to Barclay Mowlem for their fine cooperation and their approval to publish the results of the field measurements.

9 References

[1] Lodewijks, G.: The Power Consumption of Conveyor Belts (in Dutch); BULK Vol. 5 (1997), No. 2, pp. 66-74.
[2] Nordell, L.K.: The Power of Rubber – Part I; Bulk Solids Handling Vol. 16 (1996), pp. 333-340.
[3] Nordell L.K., Ciozda, Z.P.: Transient Belt Stresses During Starting and Stopping: Elastic Response Simulated by Finite Element Methods; Bulk Solids Handling Vol. 4 (1984), pp. 93-98.
[4] Lodewijks, G.: The Rolling Resistance of Belt Conveyors; Bulk Solids Handling Vol. 15 (1995), pp. 15-22.
[5] Cema: Belt Conveyors for Bulk Materials; Fifth Edition, 1997.
[6] Lodewijks, G.: Non-linear Dynamics of Belt Conveyor Systems; Bulk Solids Handling Vol. 17 (1997), pp. 57–67.